

MANEUVER LOAD ALLEVIATION OF THE DRY WING FOR HYDROGEN AIRCRAFT

Fanglin Yu[1] & Mirko Hornung[1]

[1]Chair of Aircraft Design, Technical University of Munich, Boltzmannstrasse 15, 85748 Garching b. München, Germany

Abstract

Hydrogen-powered aircraft necessitate a “dry wing” design, relocating fuel from the wings to the fuselage. This fundamental design change eliminates the beneficial inertial relief traditionally provided by wing-borne fuel, resulting in a substantial increase in structural loads and a corresponding mass penalty. This study investigates active Maneuver Load Alleviation (MLA) as a critical enabling technology to mitigate this mass penalty. A multi-fidelity aeroelastic toolchain (FAST), which is capable of aeroelastic modeling, loads analysis, and structural sizing, is employed to evaluate the effectiveness of MLA on two configurations: a current state-of-the-art reference aircraft (A320-like) and a futuristic High Aspect Ratio (HAR) aircraft. The results demonstrate that for the reference configuration, the dry wing incurs a 9.3% structural mass penalty compared to the conventional wet wing. Activating the MLA system successfully mitigates this penalty, reducing the mass increment to just 0.5%, thereby demonstrating MLA as an essential solution for the structural feasibility of hydrogen-fueled aircraft. However, for the HAR configuration, the effectiveness of the MLA system is severely limited. This limitation arises because the structural sizing of the HAR wing is largely dominated by aeroelastic constraints, specifically aileron reversal, which the active MLA system cannot alleviate. Consequently, the additional stiffness required to satisfy these constraints significantly dilutes the mass reduction benefits provided by the MLA system.

Keywords: Hydrogen Aircraft, Dry Wing, Aeroelasticity, Load Alleviation, Structural Sizing

1. Introduction

Hydrogen-powered aircraft represent a promising pathway toward sustainable air transport; however, they necessitate the "dry wing" concept, where fuel is relocated from the wings to the fuselage. This shift is driven by the limited internal wing volume, which cannot accommodate the high-capacity requirements of cryogenic liquid hydrogen. This fundamental design change eliminates the beneficial inertial relief traditionally provided by wing-borne fuel, resulting in a substantial increase in structural loads and a corresponding mass penalty. This issue is further exacerbated by the contemporary trend toward High Aspect Ratio (HAR) wings, essential for aerodynamic efficiency, which presents significant structural and aeroelastic hurdles for the aircraft design.

Within the DLR EXACT project, investigations into long-range hydrogen aircraft have highlighted these challenges. Conceptual load analyses performed with the LOADzero tool revealed that hydrogen-powered aircraft experience a 19% increase in maximum wing shear force (F_z) and a 15% increase in wing root bending moment (M_x) compared to conventional kerosene-powered configurations [1]. Furthermore, a previous study by the author quantified the impact on the wingbox internal loads, showing a 48% increase in shear force and a 25% increase in bending moment using high-fidelity methods [2].

To mitigate this load increase, active Maneuver Load Alleviation (MLA) presents a compelling solution. The concept of MLA emerged in the late 1970s and has since been a subject of rigorous

study. Early work by White explored diverse MLA configurations—including inboard flaps and outboard ailerons—demonstrating that active MLA could potentially allow for a 10% increase in wingspan without additional structural weight, leading to a 13% payload enhancement [3]. Practical flight tests on the F-111 confirmed these benefits, where load factor increases of up to $1.0\,\mathrm{g}$ were achieved without increasing wing root bending moments by utilizing flap-based MLA [4].
More recent research has expanded on these benefits at the systems and conceptual levels. Xu [5] investigated MLA on conventional transport aircraft, finding potential fuel consumption reductions of 4%. On the wing level, Handojo [6] explored the collective impact of aeroelastic tailoring, MLA, and gust load alleviation on wingbox mass. Furthermore, Binder [7] demonstrated the synergy between MLA and structural tailoring, showing that their combined application can achieve a 23% greater weight reduction than either technology alone.
Existing research suggests that MLA is a promising approach to mitigate the load increases caused by the absence of fuel inertial relief. Therefore, MLA acts as a key enabler for feasible hydrogen dry wing designs. This paper explores the application of MLA technology specifically to offset the mass penalties introduced by the hydrogen dry wing configuration, quantifying its impact through a multi-fidelity optimization framework.

2. Load Alleviation and Structural Sizing Framework

2.1 Aircraft Models

This study utilizes an A320-like configuration developed by Bauhaus Luftfahrt (BHL). Constructed primarily from aluminum, this baseline was designed using the tool Bauhaus Luftfahrt Aircraft Design Environment (BLADE), and adheres to the same top-level aircraft requirements (TLARs) as the Airbus A320, with its geometry shown in Figure 1. The reference configuration retains the control surface layout of the A320, featuring three trailing edge control surfaces per wing (one inner flap, one outer flap, and one aileron). A hydrogen-powered derivative is generated using the same tool and TLARs. This derivative adopts a dual-tank architecture, housing the liquid hydrogen in both forward and rear fuselage tanks. Although integrating a forward tank presents cabin safety and certification challenges, which fall outside the present scope, this dual-tank layout was selected to mitigate the significant Center of Gravity (CG) shifts associated with pure-aft configurations. To rigorously isolate the structural impacts of the dry wing architecture, the wing planform is kept identical to the baseline. Furthermore, the investigation is not limited to current state-of-the-art short-to-medium-range aircraft. A futuristic HAR (AR=16) configuration is also considered, which is derived under the identical TLARs by extending the wingspan and proportionally reducing the chord length. The planforms of both configurations are shown in Figure 3. For all derivative configurations, the fundamental control surface layout is maintained, with the individual control surfaces scaled proportionally according to the local span and chord dimensions.



Figure 1 – *Geometry of the reference configuration.*

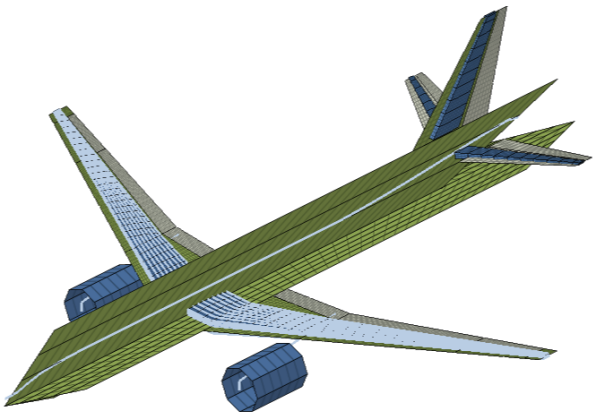


Figure 2 – *Aeroelastic model of the reference configuration.*

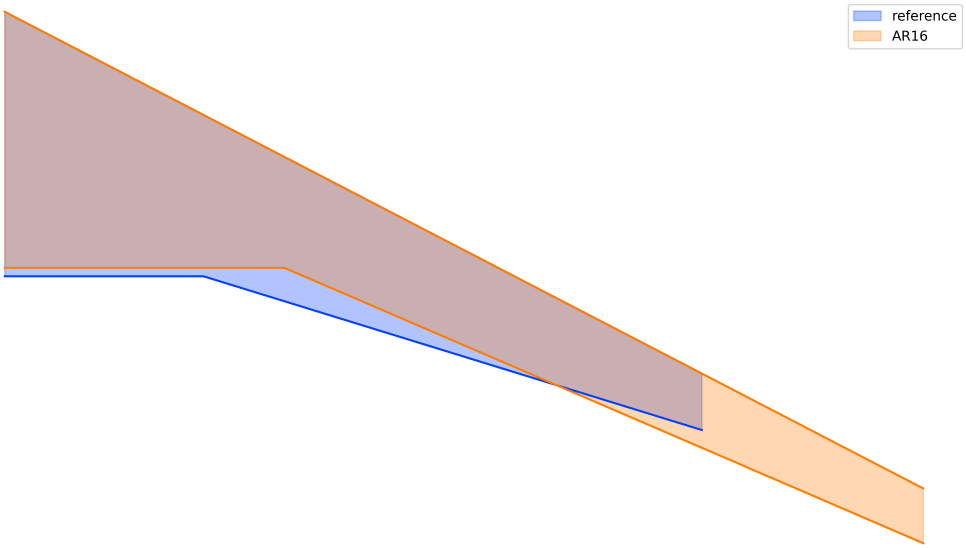


Figure 3 – *Comparison of the wing planforms.*

The aeroelastic model (Figure 2) is automatically generated using the in-house multi-fidelity toolchain, the *Flexible Aero-Structural Toolbox* (FAST) [2]. The wing structure is modeled using a Finite Element Method (FEM) approach, where shell elements represent the skins, ribs, and spars, and beam elements represent the stiffeners, stringers and engine pylons to accurately capture load paths and buckling behavior. Meanwhile, the fuselage is modeled as a rigid beam to provide necessary boundary condition and preserve computational efficiency. Aerodynamically, the configuration is modeled using the Doublet Lattice Method to compute aerodynamic loads. For comprehensive details regarding the automated model generation process, including mass modeling and aero-structural coupling, the reader is referred to this dedicated FAST publication [2].

2.2 Active Maneuver Load Alleviation

To implement MLA, the appropriate control surface scheduling must first be determined. In the current study, the active MLA system is applied exclusively to symmetrical maneuvers. To thoroughly explore the potential of MLA, all control surfaces are utilized as multifunctional control devices, capable of both upward and downward deflections.

The derivation of the optimal MLA control surface scheduling is formulated as an optimization problem:

$$\begin{aligned} &\underset{\delta_i}{\text{minimize}} \quad f(\delta_i) \\ &\text{subject to} \quad \delta_{min} \leq \delta_i \leq \delta_{max}, \quad i = 1, \ldots, 3 \end{aligned} \tag{1}$$

The design variables are the deflections δ_i of the individual control surfaces. MSC Nastran SOL 144 is utilized to compute the aeroelastic maneuver loads, and the objective function $f(\delta_i)$ is defined as the resulting wing root bending moment, as this serves as a reliable indicator of the overall maneuver loads. These design variables are bounded by their physical deflection limits (δ_{min} and δ_{max}). A sensitivity study on this maximum deflection limit is subsequently conducted to evaluate its influence on the overall system performance and load alleviation efficacy.

Due to the computational expense of optimizing the scheduling for every individual flight condition, the optimal control surface deflections are derived exclusively for the critical sizing load cases identified during the load analysis. Once the optimal scheduling for these critical cases is established, a linear scaling approach is applied to all other operational conditions. Specifically, the MLA system remains inactive during unaccelerated level flight (load factor $n_z = 1$). For all other maneuvering conditions, the control surface deployment is scaled proportionally to the commanded load factor.

2.3 Loads Analysis

To rigorously evaluate the efficacy of the load alleviation technology, a comprehensive aeroelastic load analysis is conducted both with and without the MLA system active. In accordance with CS-25 certification requirements [8], the simulations encompass a representative set of symmetric (pull-up and push-over) and asymmetric (roll) maneuvers across various speeds, altitudes, and load factors. Furthermore, the analysis accounts for multiple mass configurations by incorporating diverse combinations of payload and fuel, with the CG spanning from 15% to 40% of the mean aerodynamic chord [9].

The simulation results are post-processed to construct 1D spanwise load envelopes. These envelopes encapsulate the absolute maximum and minimum internal forces—specifically shear force, bending moment, and torsional moment—encountered at each spanwise station across all simulated flight conditions. The two distinct critical load sets, representing the baseline and the MLA-alleviated conditions, are subsequently employed in the structural sizing stage to quantify the mass savings enabled by the technology.

2.4 Structural Sizing

To evaluate the impact of MLA on wing mass, a two-stage structural optimization is performed using the MSC Nastran SOL 200 module. The primary objective is to minimize the wingbox mass by optimizing the thicknesses of the skins, spars, and ribs across each rib bay. The stiffeners and stringers are pre-sized analytically and held constant during the optimization. Although this approach does not fully exploit the potential of the optimization, it avoids a drastic increase in the number of design variables and computational time. The first stage minimizes mass subject to material strength (applying a safety factor of 1.5 to the ultimate von Mises stress) and structural buckling (enforcing an eigenvalue $\lambda \geq 1.4$ across the first ten modes). Although only the lowest mode determines the critical buckling load, enforcing this constraint across the first ten modes prevents mode switching during the optimization process. A second stage is subsequently initiated if the design violates the aileron effectiveness criterion ($\eta = -\frac{Cl_{\delta_a}}{Cl_p} > 0$). This aileron effectiveness is calculated as the ratio of the roll coefficient derivative with respect to aileron deflection to the roll damping coefficient. In this stage, the optimized thicknesses from the first stage serve as lower bounds, ensuring any additional mass is strictly driven by aeroelastic control requirements.

This FEM-based framework yields the theoretical optimal mass of the primary wingbox structure [9]. Non-optimal factors, such as joints and fasteners, alongside secondary masses, are excluded from the optimization and incorporated empirically. Finally, to quantify the structural benefits, this comprehensive sizing procedure is executed for both the MLA-enabled and MLA-inactive load envelopes.

3. Sensitivity Analysis of Control Surface Layout and Deflection Limits

To investigate the influence of the control surface layout on the potential for MLA, the total number of control surfaces was increased. The initial trailing-edge layout was subdivided to derive a new configuration, as illustrated in Figure 4. This extended setup theoretically provides greater degrees of freedom to tailor the aerodynamic load distribution along the wingspan.

As outlined in Section 2.2, an optimization framework was employed to determine the ideal control surface scheduling. A $2.5\,\mathrm{g}$ pull-up maneuver was simulated. The optimization revealed a distinct deflection pattern: the two innermost control surfaces (corresponding to the original inner flap) deflected downwards to their maximum limit, whereas all remaining outboard surfaces deflected upwards to their limits. This differential scheduling effectively shifts the lift distribution inboard.

In addition to the $2.5\,\mathrm{g}$ pull-up, a $-1.0\,\mathrm{g}$ push-over maneuver was simulated, exhibiting a similarly constrained, binary deflection phenomenon. The preliminary results highlight that effective MLA fundamentally requires control surfaces capable of maximum deflection in both directions.

This analysis was also extended to the hydrogen-powered aircraft. Although the hydrogen variant exhibits a distinctly different spanwise loading distribution—primarily due to the lack of wing fuel inertial relief—it demonstrates an identical control surface scheduling behavior.

These collective results indicate that increasing the number of control surfaces beyond the baseline layout does not yield additional load alleviation benefits for these critical flight cases. The control

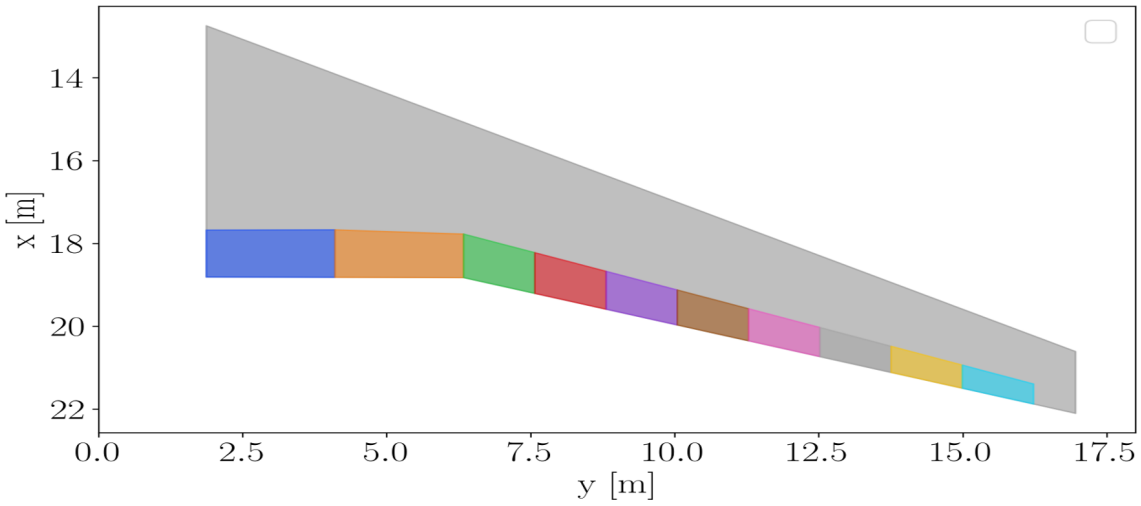


Figure 4 – *Extended layout with 10 control surfaces.*

surfaces simply saturate at their physical limits, and no intermediate differentiation in deflection angles was observed. Consequently, the subsequent analyses in this study will maintain the initial three-surface configuration.

However, it should be noted that because only a limited set of critical flight conditions was simulated, the spanwise location where the control surface deflections transition from downward to upward (the split point) may vary. Therefore, the optimal control surface layout may ultimately depend on tracking this variable split point across a broader range of flight conditions in future work.

A sensitivity analysis was conducted to evaluate how the maximum control surface deflection limit influences the efficacy of MLA. As illustrated in Figure 5, a linear relationship is observed between the maximum deflection limit and the wing root bending moment. This behavior is expected, given that the aerodynamic solver in MSC Nastran relies on linear potential flow theory. Consequently, localized nonlinear aerodynamic phenomena—such as control surface stall at high deflection angles—cannot be captured by this approach. While accurately resolving these stall effects would require high-fidelity Computational Fluid Dynamics analyses, such investigations fall outside the scope of the present study. To ensure realistic aerodynamic boundaries, the maximum deflection limit is instead established based on existing literature. Following the reference work by Xu [5], the maximum allowable control surface deflection is set to $20\,\mathrm{deg}$.

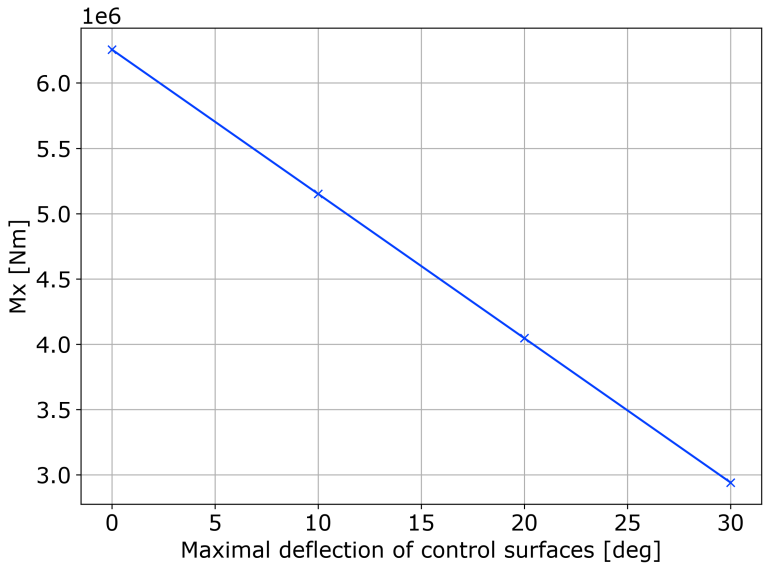
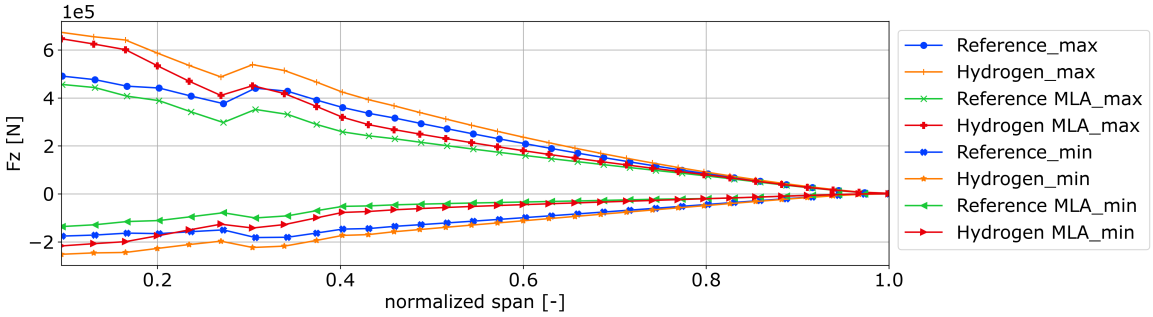


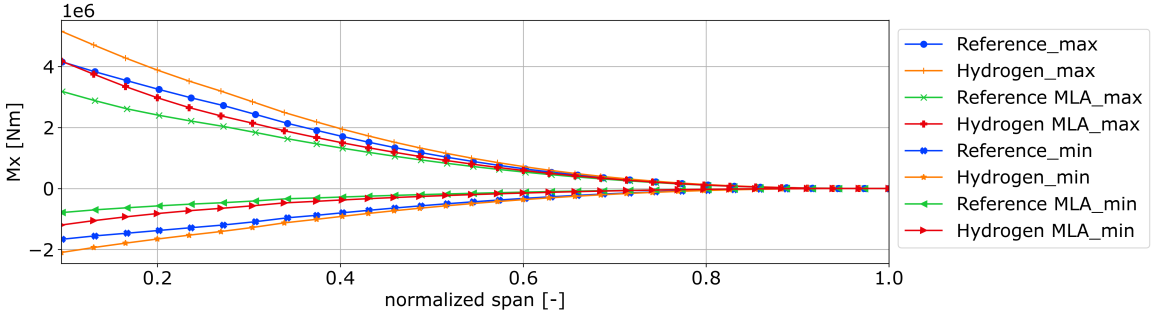
Figure 5 – *Sensitivity of the wing root bending moment to maximum deflection limits.*

4. Effectiveness of MLA on the Reference Aspect Ratio Configurations

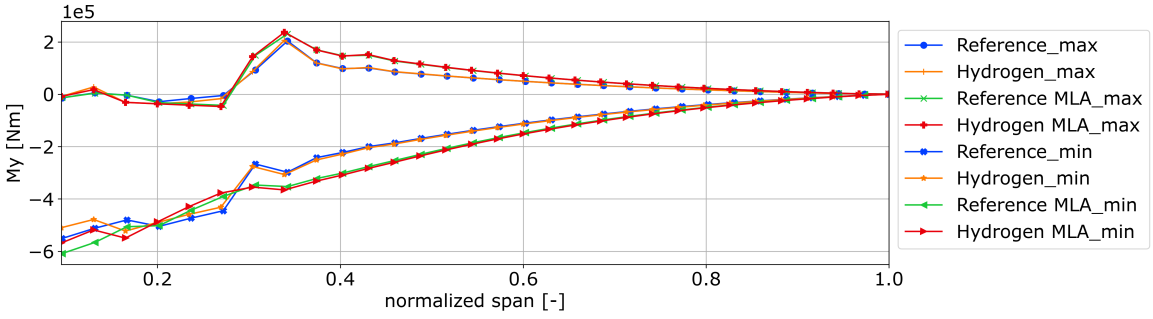
Having determined the optimal control surface scheduling and established the maximum deflection limit, comprehensive aeroelastic load analyses were executed across all operational flight conditions. Figure 6 presents the resulting load envelopes, comparing the reference wet wing and the baseline dry wing configurations, both with and without the active MLA system. In Figure 6a, a distinct load reduction is visible at a normalized span location of approximately 2.7, caused by the inertial relief of the engine and pylon. As illustrated by the spanwise bending moment distribution in Figure 6b, the baseline dry wing exhibits a significant increase of approximately 24% in the maximum bending moment compared to the wet wing. Crucially, activating the MLA system successfully mitigates this increase, reducing the positive bending moment to a level comparable to the original reference aircraft, while further decreasing the negative bending moment by 28%. However, as shown in Figure 6c, the MLA system slightly increases the torsional moment along the outboard wing section. For example, during a pull-up maneuver, the outboard flap and aileron are deflected upwards to alleviate bending loads. This upward deflection effectively creates a reflex airfoil profile, generating a nose-up aerodynamic pitching moment that directly increases the structural torsional loads. Regarding the critical load cases that constitute the load envelope, the MLA system introduces roll maneuvers as a new sizing condition. This shift occurs because the symmetrical maneuver loads are effectively alleviated, allowing roll maneuvers, which previously did not dictate the load envelope, to become dominant.



(a) Shear force



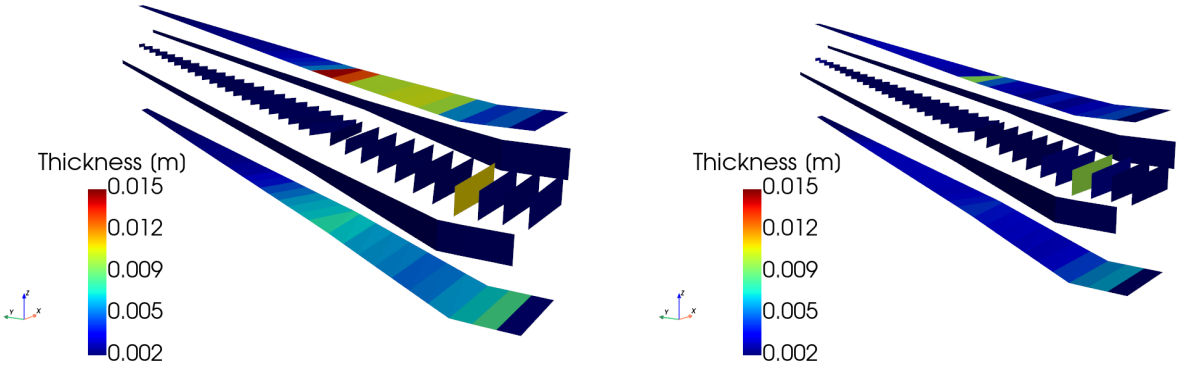
(b) Bending moment



(c) Torsional moment

Figure 6 – *Comparison of load distributions for the reference aspect ratio configuration.*

Figure 7 displays the thickness distribution of the wingbox for the LH2 aircraft both with and without MLA, demonstrating that implementing this system allows for a significant overall reduction in structural thickness. Table 1 summarizes the wingbox mass results derived from the FEM-based sizing for all configurations with the reference aspect ratio (AR). This quantification highlights the substantial benefit of MLA technology, yielding a 4.8% mass reduction for the kerosene aircraft and an 8.0% mass reduction for the hydrogen aircraft. Without MLA, the dry wing configuration incurs a structural mass penalty of 9.3% compared to the conventional wet wing. However, the activation of the MLA system significantly mitigates this penalty, reducing the mass increment to only 0.5%, as evidenced by comparing the dry wing with MLA ($9530\,\mathrm{kg}$) directly to the reference wet wing ($9478\,\mathrm{kg}$).



(a) no MLA (b) with MLA

Figure 7 – *Thickness distribution of wingbox for the reference aspect ratio LH2 aircraft.*

Table 1 – Wing Mass Comparison of reference aspect ratio configurations

Configurations	No MLA	MLA	Percentage [−]
Wet wing	9478 kg	9021 kg	−4.8%
Dry wing	10357 kg	9530 kg	−8.0%
Percentage [-]	9.3%	5.6%	

5. Effectiveness of MLA on the HAR Configurations

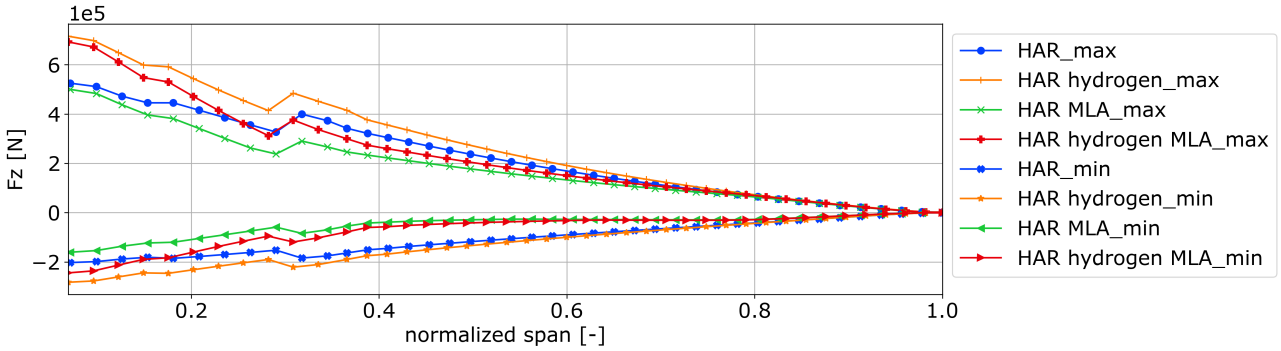
The same study was conducted on the HAR wing. The results of loads analysis are shown in Figure 8. Similar to the observations for the reference AR, the hydrogen wing exhibits a substantial load increase of approximately 26% in bending moment compared to the wet wing. With the activation of the MLA system, this load can be reduced to a level comparable to the wet wing. Furthermore, the critical load cases follow a similar trend as the reference AR, with roll maneuvers emerging as new sizing conditions.

The structural sizing procedure was subsequently repeated for the HAR wing, with the resulting wing masses summarized in Table 2. In contrast to the reference AR configuration, the MLA system yields a relatively modest mass reduction of only 2.1% for both the wet and dry wing configurations.

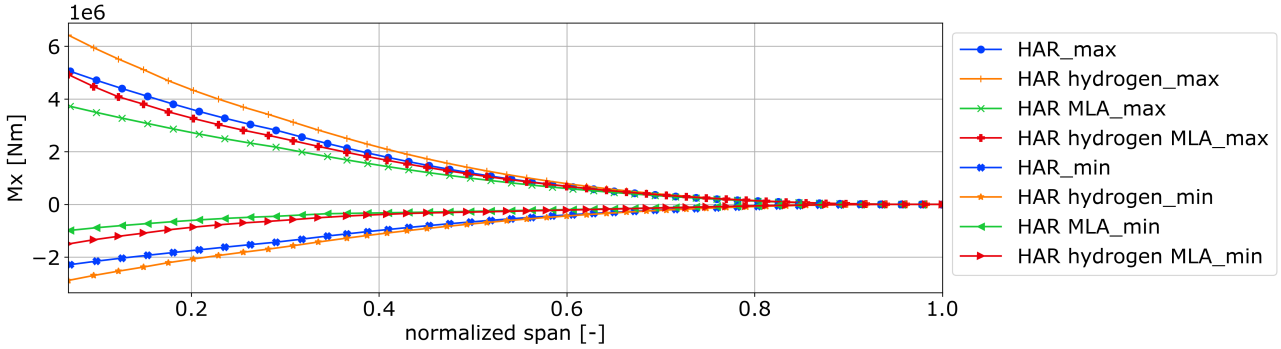
Table 2 – Wing Mass Comparison of HAR configurations

Configurations	No MLA	MLA	Percentage [−]
Wet wing	15360 kg	15032 kg	−2.1%
Dry wing	16749 kg	16400 kg	−2.1%
Percentage [-]	9.0%	9.1%	

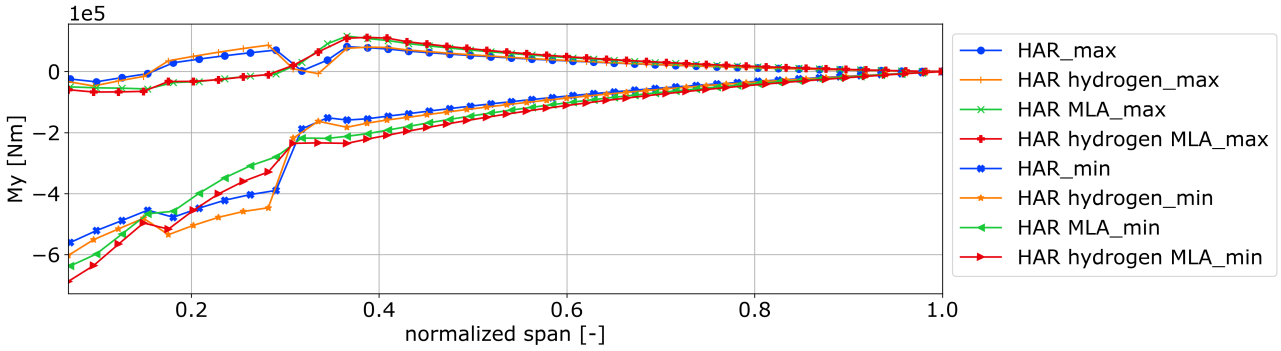
Examining the details of the structural sizing, Figure 9 illustrates the thickness distribution of the HAR



(a) Shear force



(b) Bending moment



(c) Torsional moment

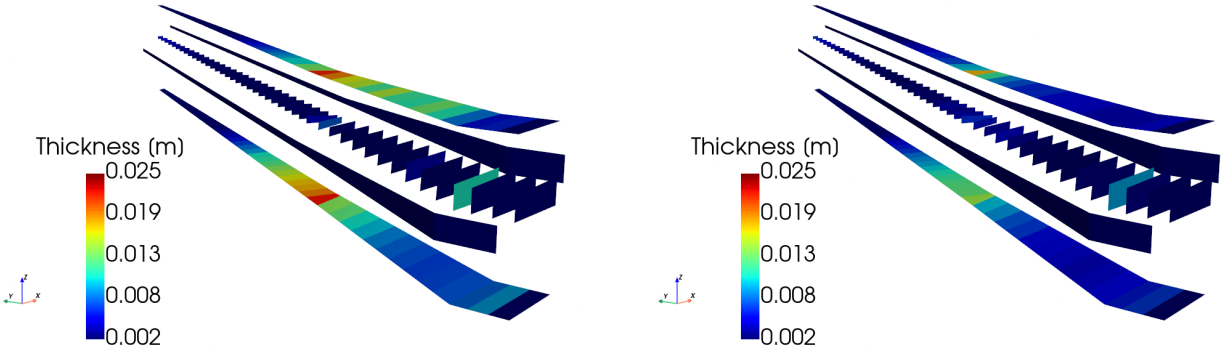
Figure 8 – *Comparison of load distributions for the HAR configuration.*

wing at the first sizing stage, which exclusively considers material strength and buckling constraints. It is evident that the MLA system effectively reduces the required structural thickness. Table 3 summarizes the corresponding wing mass comparison for the HAR configurations at this stage. The data demonstrates that the MLA system substantially reduces the mass of the dry wing, which directly correlates with the drastic load alleviation previously shown in Figure 8. This confirms the effectiveness of the MLA system, yielding a mass reduction of approximately 12.4% for the wet wing and 11.4% for the dry wing. Furthermore, the hydrogen HAR wing equipped with the active MLA system completely mitigates the dry wing mass penalty when compared to the conventional wet HAR wing.

Table 3 – Wing Mass Comparison of HAR configurations no aeroelastic constraints

Configurations	**No MLA**	**MLA**	**Percentage [−]**
Wet wing	12 183 kg	10 673 kg	−12.4%
Dry wing	13 690 kg	12 131 kg	−11.4%
Percentage [-]	12.4%	13.7%	

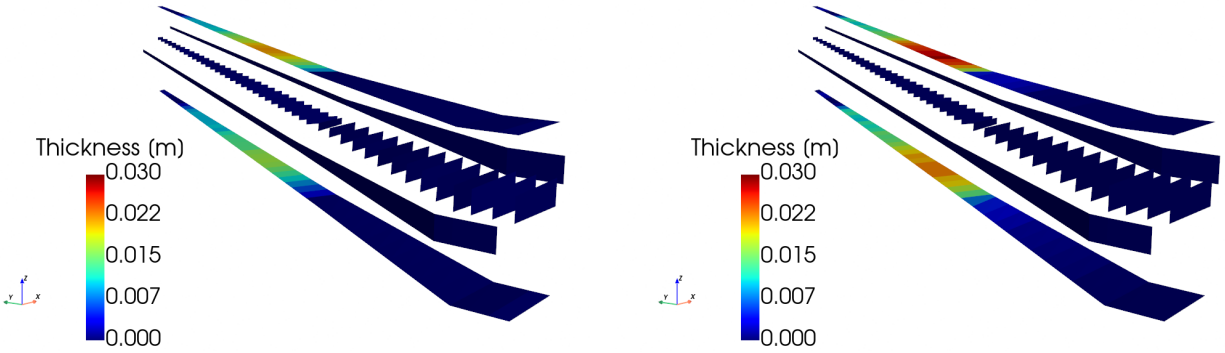
However, the second stage of the structural sizing introduces aeroelastic constraints, specifically



(a) no MLA (b) with MLA

Figure 9 – *Thickness distribution of wingbox for the HAR LH2 aircraft at the first stage structural sizing.*

aileron reversal. The wing thickness is drastically increased during this second stage due to these aeroelastic constraints, which the MLA system cannot alleviate. In contrast, the MLA system increases the torsional moment at the outboard section, as indicated in Figure 8c, further exacerbating the situation. This required additional thickness is illustrated in Figure 10. Compared to the inactive MLA case, the active MLA configuration requires significantly more stiffening. This occurs because the initial wing structure from the first stage is sized for the alleviated bending loads, as shown in Figure 9, and must simultaneously withstand the higher torsional moments induced by the active MLA system. Consequently, the thickness increase during the second stage is far more significant for the MLA case, as shown in Figure 10b. This requirement for additional stiffness severely dilutes the mass reduction benefits provided by the MLA system at the first sizing stage.



(a) no MLA (b) with MLA

Figure 10 – *Additional thickness added to the wingbox for the HAR LH2 aircraft at the second stage structural sizing.*

6. Conclusions

This study employs high-fidelity aeroelastic simulations and optimization methodologies to assess the impact of MLA on a current state-of-the-art reference aircraft (A320) and a futuristic HAR aircraft. The results indicate that the hydrogen-powered wing experiences significant load increases and mass penalties. However, for the reference AR configuration, the MLA system can effectively mitigate

these load increases and their associated mass penalties. The results presented herein validate the effectiveness of the MLA system in successfully compensating for the significant loss of inertial relief, which is inherent in the structural design of hydrogen aircraft. By limiting the overall structural mass penalty to approximately 0.5%, MLA is confirmed as a key enabling technology for the structural feasibility of hydrogen-fueled aircraft. Conversely, the effectiveness of the MLA system is severely limited for the HAR configuration. The primary reason for this limitation is that the structural sizing of the HAR wing is largely dominated by aeroelastic constraints, which the MLA system cannot alleviate. Instead, it exacerbates the situation by increasing the torsional loads.

7. Outlook

The current MLA design is exclusively applied to symmetrical maneuvers, which inadvertently shifts the critical sizing conditions to certain roll maneuvers. Therefore, future work should extend the MLA framework to actively alleviate loads during these roll maneuvers. Additionally, the present study assumes that nonlinear aerodynamic effects are neglected at high control surface deflections. This assumption requires rigorous verification in subsequent investigations, as such nonlinearities could potentially diminish the predicted benefits of the MLA system. Further studies must also be conducted specifically on the HAR wing. For instance, the control surface layout could be optimized to mitigate the significant aeroelastic constraints encountered during the structural sizing process. Overcoming these constraints would ensure that the sizing remains dominated by structural loads, thereby allowing the MLA system to demonstrate its full effectiveness. Moreover, the inclusion of gust and landing loads is essential to complete the load analysis, providing a comprehensive load envelope and enabling the assessment of the MLA system under more extensive operational conditions. Furthermore, alongside active MLA systems, composite materials could be utilized to achieve passive maneuver load alleviation, fully exploiting the synergistic potential for load alleviation. Finally, as the present assessment focuses exclusively on the wing level, these structural sizing results will be fed back into the overall aircraft design process to systematically evaluate their cascading effects on the entire aircraft.

8. Acknowledgements

The work presented has been conducted within the framework of project DWiTE (grant agreement No. 20M2247D) funded by the Federal Ministry for Economic Affairs and Climate Action of Germany. The authors thank Alexandros Lessis from Bauhaus Luftfahrt for his valuable support in providing the CPACS data for the aircraft configuration.

9. Contact Author Email Address

To contact the author, please use the following email address: fanglin.yu@tum.de

10. Copyright Statement

The authors confirm that they, and/or their company or organization, hold copyright on all of the original material included in this paper. The authors also confirm that they have obtained permission, from the copyright holder of any third party material included in this paper, to publish it as part of their paper. The authors confirm that they give permission, or have obtained permission from the copyright holder of this paper, for the publication and distribution of this paper as part of the ICAS proceedings or as individual off-prints from the proceedings.

References

[1] Hecken T, Balack P, Atanasov G, Silberhorn D, Petsch M, and Zerbst D. Conceptual Loads Assessment of Aircraft with Fuselage Integrated Liquid Hydrogen Tank. In *DLRK*, 2022.

[2] Yu F, Sebastia Saez C, and Hornung M. A Multi-Fidelity Aeroelastic Toolchain: From UAVs to Hydrogen Transport Aircraft. *Aerospace*, 13(3):286, March 2026. https://doi.org/10.3390/aerospace13030286.

[3] White R J. Improving the Airplane Efficiency by Use of Wing Maneuver Load Alleviation. *Journal of Aircraft*, 8(10):769–775, October 1971. https://doi.org/10.2514/3.59169.

[4] Thornton V. Reduction of Structural Loads Using Maneuver Load Control on the Advanced Fighter Technology Integration (AFTI)/F-111 Mission Adaptive Wing. Technical report, 1993.

[5] Xu J and Kroo I. Aircraft Design with Maneuver and Gust Load Alleviation. In *29th AIAA Applied Aerodynamics Conference*, Honolulu, Hawaii, June 2011. https://doi.org/10.2514/6.2011-3180.

[6] Handojo V, Lancelot P, and De Breuker R. Implementation of Active and Passive Load Alleviation Methods on a Generic mid-Range Aircraft Configuration. In *2018 Multidisciplinary Analysis and Optimization Conference*, Atlanta, Georgia, June 2018. https://doi.org/10.2514/6.2018-3573.

[7] Binder S, Wildschek A, and De Breuker R. The Interaction Between Active Aeroelastic Control and Structural Tailoring in Aeroservoelastic Wing Design. *Aerospace Science and Technology*, 110:106516, March 2021. https://doi.org/10.1016/j.ast.2021.106516.

[8] EASA. Certification Specification 25, 2023.

[9] Yu F and Hornung M. Aeroelastic Evaluation of Dry Wing Effects for Hydrogen Aircraft. In *CEAS*, 2025.